Supplementary Information for

Solution-Phase Synthesis of the Chalcogenide Perovskite Barium Zirconium Sulfide as Colloidal Nanomaterials

Daniel Zilevu, Omri O. Parks, and Sidney E. Creutz*

Table of Contents.

General Experimental Methods	.....	*S2*
Synthetic Procedure	.....	*S3*
Additional Reaction Data under Various Conditions	.....	*S5*
Rietveld Refinement	.....	*S13*
Electron Diffraction Data	.....	*S15*
Lattice Fringes Observed by TEM	.....	*S17*
Additional PDF Data and Information	.....	*S18*
Supplemental References	.....	*S19*

Experimental Methods.

General Synthetic Considerations. All synthetic manipulations were carried out under an atmosphere of ultrapure argon or dinitrogen gas in a glove box or using a Schlenk line unless otherwise stated. $Ba[N(SiMe_3)_2]_2(THF)_2$ was synthesized according to previous reports, recrystallized from pentane, and stored in an N_2 glovebox.[1–3] Tetrakis(dimethylamido)zirconium was purchased from Sigma-Aldrich, stored in an N2 glovebox, and purified by sublimation before use. N,N'-Diethylthiourea was purchased from Alfa Aesar and purified by recrystallization from benzene, followed by drying at 60 oC in vacuo overnight, prior to use. Oleylamine (70%) was purchased from Sigma-Aldrich and refluxed in vacuo at 120 ^oC over CaH_2 for two hours before distilling in vacuo, then stored over 4 Å molecular sieves in an N_2 glovebox prior to use. For workups carried out in the glovebox, ethanol was dried by distilling from magnesium, and chloroform was dried by passing over activated alumina and stored over molecular sieves.

Powder X-ray Diffraction. Samples for powder X-ray diffraction were dropcast from solution onto a zero-background silicon plate. PXRD data was collected using Cu K_α radiation with an AXRD Benchtop diffractometer from Proto Manufacturing equipped with a Dectris MYTHEN2 R 1D hybrid photon-counting detector in Bragg-Brentano geometry. The step size was 0.020^o and dwell times between 5-15 seconds were used, with a 1 mm collimating slit. Rietveld refinement was carried out in GSAS-II. Instrument parameters were determined by fitting the data from an LaB_6 standard.

Synchrotron X-ray Scattering and PDF analysis. Samples for synchrotron X-ray analysis were prepared by packing the nanocrystal powder into a 1 mm inner diameter Kapton capillary sealed with epoxy. X-ray total scattering data was obtained *via* the mail-in program at beamline 11-ID-B at Argonne National Lab. A CeO_2 standard was used for calibration and a measurement on an empty Kapton tube was used for background subtraction. Data reduction was carried out using GSAS-II and PDF analysis and refinement was carried out using PDFfit2 *via* PDFgui.[4]

TEM and EDX Analysis. Samples for TEM were dispersed at low concentration in chloroform by sonicating for several minutes, then a drop of the resulting colloidal dispersion was allowed to air-dry on a carbon-coated copper TEM grid. Samples were dried in a vacuum dessicator overnight prior to analysis. Sample preparation was carried out in air. Imaging was performed using a JEOL 2100 TEM operating at 200 kV, and an Oxford EDS system was used for EDS analysis.

ICP-MS Analysis. The BaZrS3 samples were washed (through sonication and centrifugation) three times with 5 ml of chloroform to fully remove the excess ligands from the nanocrystals; the precipitated nanocrystals were dried in a stream of air. A mixture of HNO3, HCl, and HF in the ratio of 3:1:1 was added to the dried powder samples and placed in a hot water bath for 2 hours. After two hours of digestion, the acidified samples were diluted to 100 ml with ultrapure deionized water in a volumetric flask. A calibration curve was created using

commercially available Zr4+ and Ba2+ standards, and analysis was performed using a Perkin Elmer ELAN DRC II instrument. *Caution! Hydrofluoric acid is extremely toxic and corrosive; it should only be handled by individuals specifically trained in its use, using appropriate personal protective equipment, and in an efficient fume hood. Appropriate first aid should be readily available when HF is in use and if any exposure to vapor or liquid occurs, treatment should be started immediately.*[5]

Environmental Stability Tests. Stability was tested in air by allowing a sample deposited on a zero-background silicon plate (for PXRD analysis) to sit under room air and room light for up to 9 weeks. The ambient humidity during this time was approximately 40 ±10 %. Water stability was tested by taking a similarly deposited sample and submerging the plate in deionized water.

$BaZrS_3$ Nanomaterial Synthesis (standard protocol): In a glovebox, 1.0 g (1.23 mL) of dry oleylamine was used to dissolve 60.8 mg (0.1 mmol) of the $Ba[N(TMS)_2]_2[THF]_2$ in a scintillation vial, then this mixture was added to 53.8 mg (0.2 mmol) of the $Zr[N(CH_3)_2]_4$ in a separate vial. The metal precursor solution was transferred to a Schlenk reaction tube with a sidearm sealed with a Teflon valve and equipped with a Teflon-coated magnetic stir bar. Then, 0.8 g (6 mmol) of solid N,N′-diethyl thiourea was added to the flask and the mixture was stirred for three mins. The flask was brought outside the glovebox, the sidearm of the Schlenk tube was connected to an inert gas manifold using rubber tubing, and the Teflon valve was opened slightly. The bottom half of the flask was wrapped in a fiberglass heating tape controlled by a J-KEM PID temperature controller and heated rapidly to 365 degrees; this corresponds to the boiling point of oleylamine, and solvent can be observed refluxing on the sides of the flask. This temperature was maintained for 30 mins, then the flask was allowed to cool to room temperature. The sealed flask was then brought back into the glovebox for workup. To separate the $BaZrS_3$ nanocrystals, about 5 ml each of ethanol and chloroform were added to the crude product and stirred vigorously. The mixture was transferred to two test tubes and separated by centrifugation at 2800 rpm. The supernatant was discarded, and the precipitate was again washed with an additional 5 ml of ethanol. The supernatant was once again discarded, and the precipitate was suspended in chloroform. A typical reaction provided approximately 48% yield by mass of thoroughly washed and dried nanocrystalline precipitate (assuming all mass corresponds to $BaZrS_3$).

The dispersability and colloidal stability of the HT-$BaZrS_3$ particles can be improved by adding 200 µL of oleic acid before the first centrifugation, if needed.

Caution! Heating reaction mixtures at high temperatures presents a potential fire risk and should be carried out with caution by trained personnel, and appropriate fire safety equipment should be readily available. Ensure that the reaction vessel is opened slightly to an inert-atmosphere manifold to avoid excessive pressure build-up. Although we have not experienced any issues when the reaction is performed as described above, carrying out the reaction behind a safety shield is recommended out of an abundance of caution.

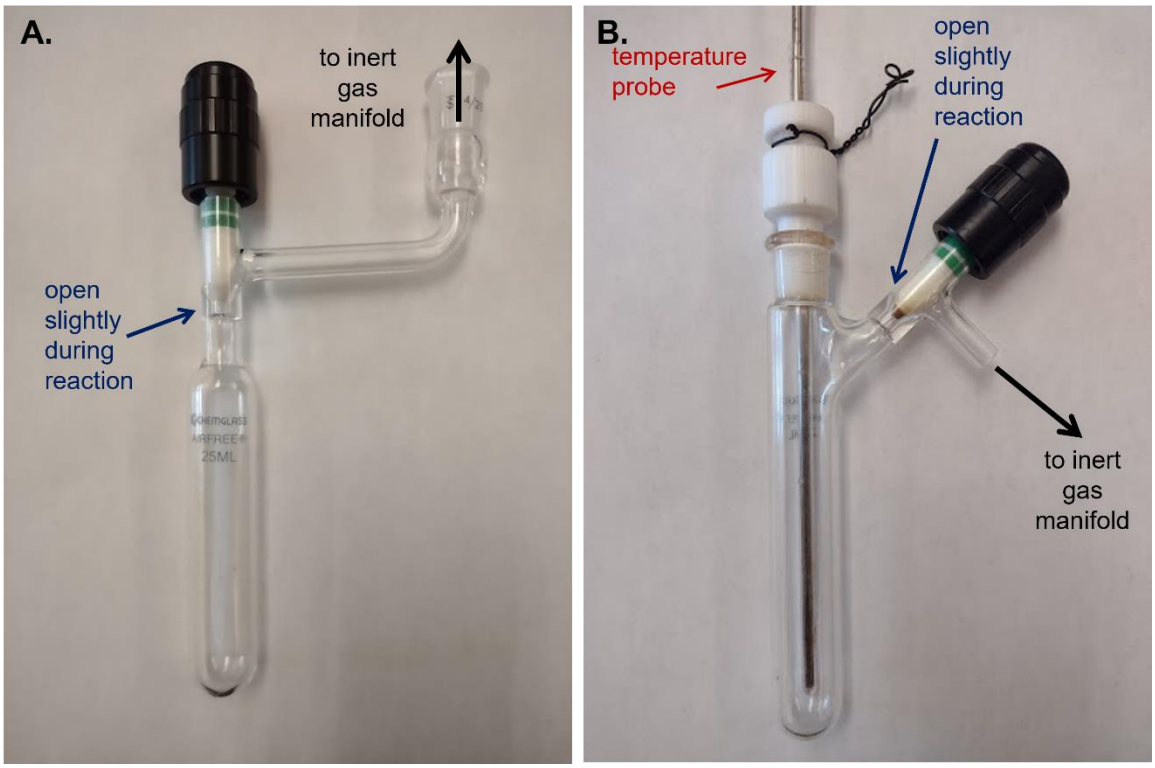

Figure S1. Two slightly different glassware setups have been used for reaction, and both give similar results. Glassware A was used for most reactions; in this case the temperature probe is secured against the exterior surface of the glass (see below). Glassware B allows for the temperature to be measured internally using a glass-sheathed immersed temperature probe; see previous report for more information.[6]

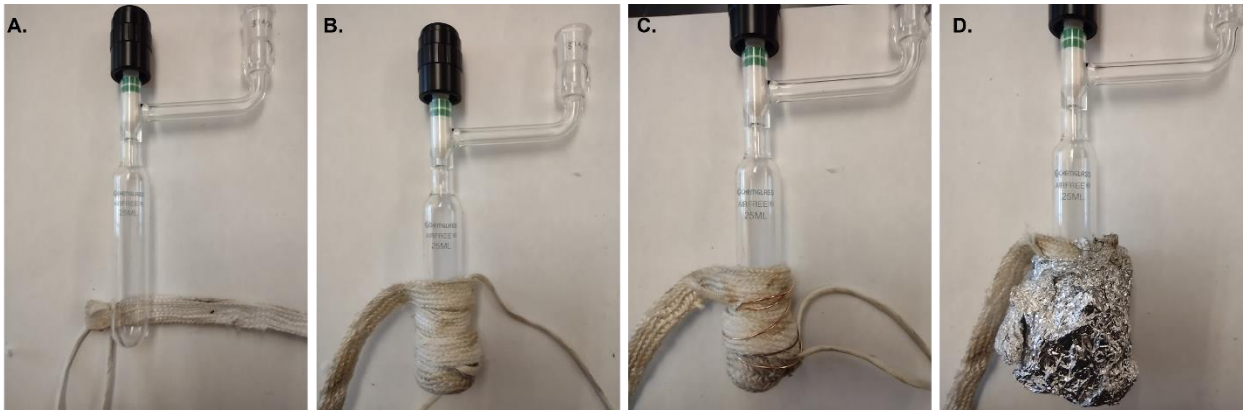

Figure S2. Heating was accomplished using a Fisherbrand fiberglass insulated heating tape (A). This is wrapped around the bottom half of the reaction tube, leaving the top open to allow internal reflux of the solvent (B). This is secured in place using copper wire (C) and further secured by wrapping with aluminum foil (D). Temperature probe is wrapped inside the heating tape against the surface of the glass.

Failed Synthetic Attempts

For reference, we include in the table below (Table S1) a description of some our attempts to prepare $BaZrS_3$ using other precursors, and the results observed. Other prior synthetic attempts have been reported by Nag *et al.*[7]

Table S1. Synthesis Attempts with Different Precursors

Precursors	Reaction Conditions	Results/Observations
$Ba(OAc)_2$, Zr(acac), S_8	Oleic acid, octadecene, 300 ^oC	Unidentified nanocrystalline products; no $BaZrS_3$
$Ba(OAc)_2$, Zr(acac), $(Me_3Si)_2S$	Oleic acid, dodecanethiol, 300 ^oC	Gray precipitate; unidentified nanocrystalline products; no $BaZrS_3$
$BaCl_2$, $ZrCl_4$, S_8	Oleylamine, 240 ^oC	No crystalline product
$BaCl_2$, $ZrCl_4$, CS_2	Oleylamine, dodecanethiol, 240 ^oC	No crystalline product

Additional Data for $BaZrS_3$ Samples Synthesized under Different Conditions

For reference, we include data from reactions carried out under a range of tested conditions, including different stoichiometries, concentrations, and temperatures. The table below (Table S2) serves as an index for these reactions, and corresponding data is shown in Figures S3 through S9. Data from three additional samples of HT-$BaZrS_3$ synthesized using the standard protocol are included (Figures S3-S5) to demonstrate the degree of reproducibility of this synthesis. For ease of reference, the samples are assigned an arbitrary reference code in the table below.

Table S2. Reaction Conditions for $BaZrS_3$ Synthesis Examples

Sample	Deviation from Standard Conditions	Results/Observations	Data Figure
SI-A	none	HT-$BaZrS_3$	S3
SI-B	none	HT-$BaZrS_3$	S4
SI-C	none	HT-$BaZrS_3$	S5
SI-D	more dilute: 3 g of oleylamine instead of 1 g	LT-$BaZrS_3$ with impurities	S6
SI-E	2 g of oleylamine	LT-$BaZrS_3$	S7
SI-F	3 g of oleylamine	LT-$BaZrS_3$ with impurities	S7
SI-G	350 ^oC	LT-$BaZrS_3$	S8
SI-H	340 ^oC	LT-$BaZrS_3$	S8
SI-I	300 ^oC	LT-$BaZrS_3$	S8
SI-J	275 ^oC	LT-$BaZrS_3$	S8
SI-K	250 ^oC	No crystalline product	S8
SI-L	1:1:30 Ba:Zr:S mole ratio	LT-$BaZrS_3$	S9
SI-M	1:1.3:40	LT-$BaZrS_3$	S9

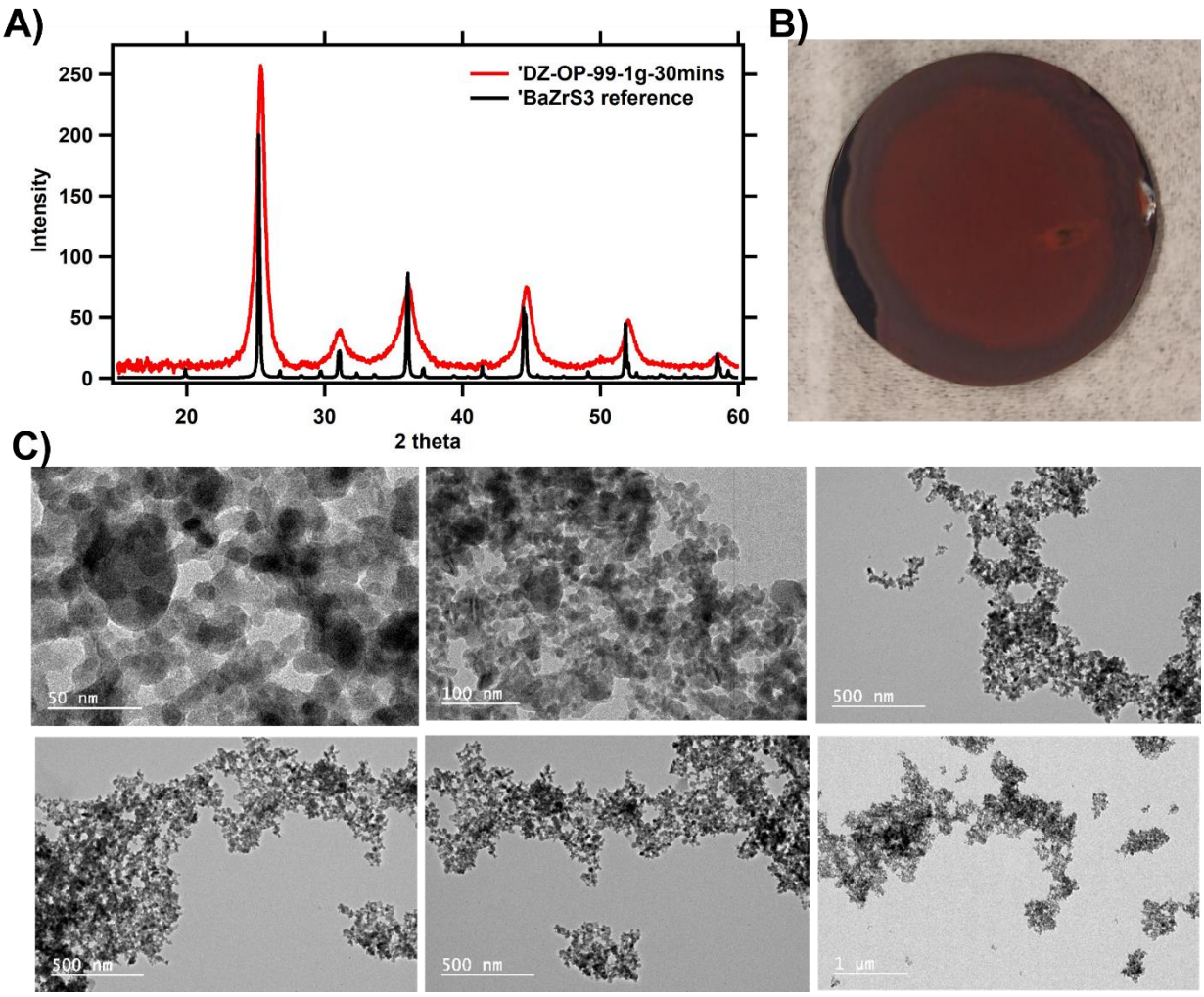

Figure S3. Characterization data for an additional sample (Sample SI-A) synthesized at the high temperature limit under standard conditions. (A) PXRD data compared to reference pattern for $BaZrS_3$ (B) Photograph of a dropcast powder of the nanomaterials (C) TEM images of the nanoparticles, with various magnifications as shown by the scale bars in the images. EDX analysis of this material gave a percent atomic composition of 62% S, 22% Ba, and 16% Zr.

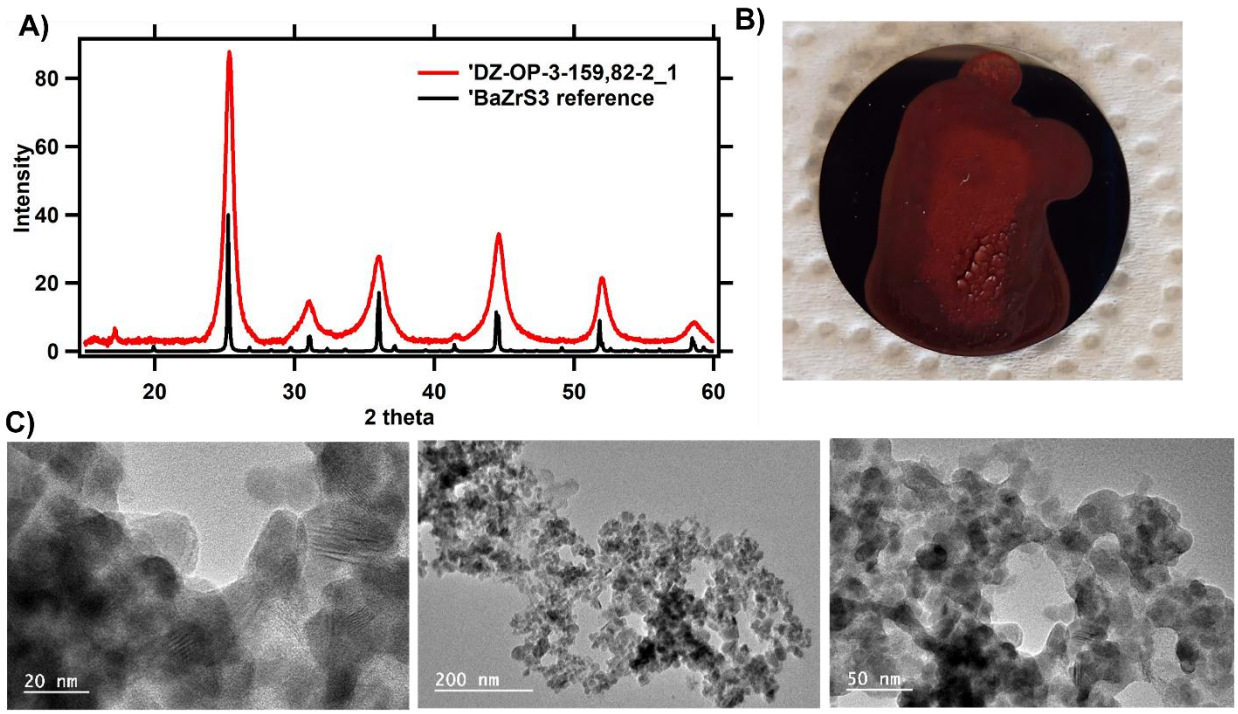

Figure S4. Characterization data for an additional sample (Sample SI-B) synthesized at the high temperature limit under standard conditions. (A) PXRD data compared to reference pattern for $BaZrS_3$ (B) Photograph of a dropcast powder of the nanomaterials (C) TEM images of the nanoparticles, with various magnifications as shown by the scale bars in the images.

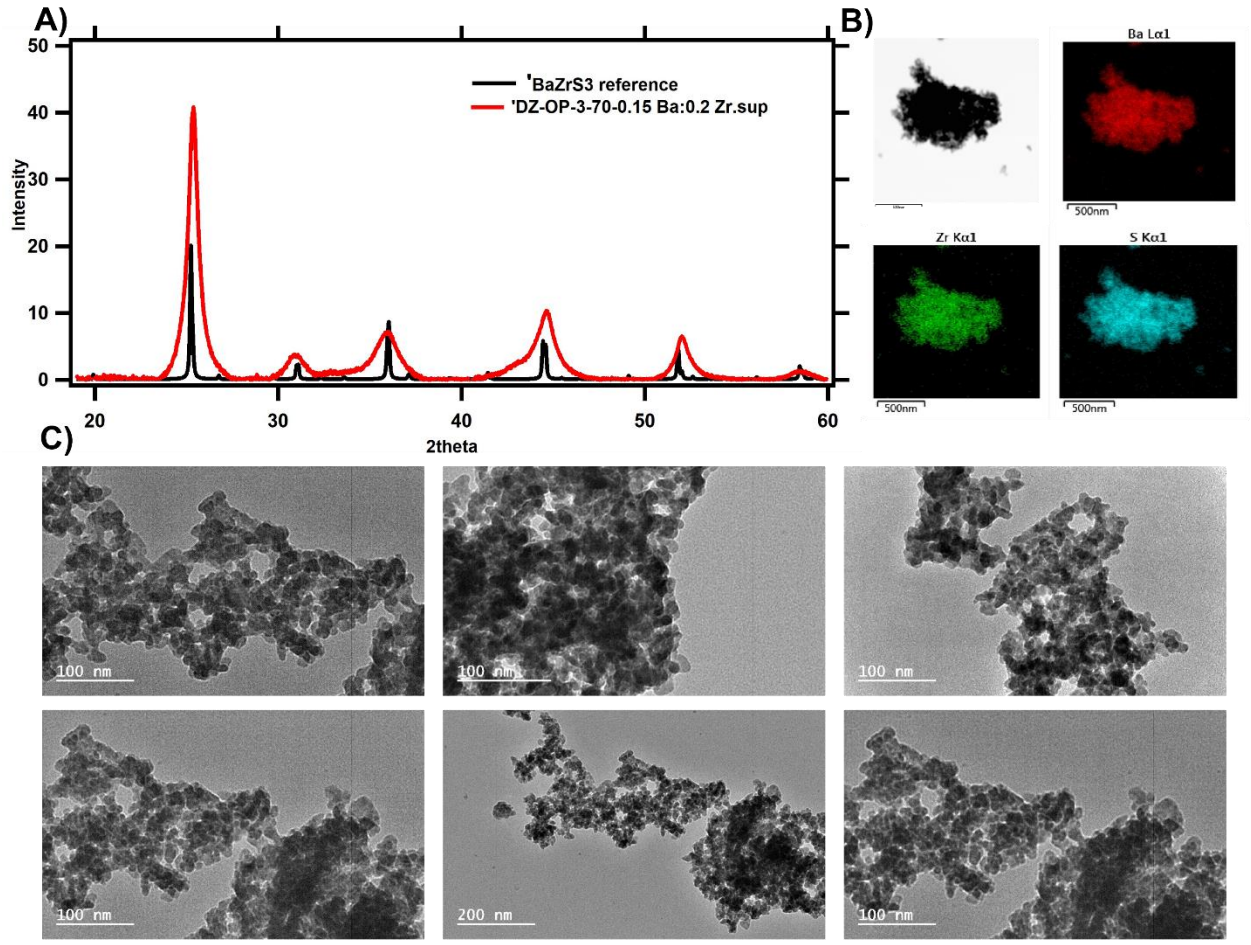

Figure S5. Characterization data for an additional sample (Sample SI-C) synthesized at the high temperature limit under standard conditions. (A) PXRD data compared to reference pattern for $BaZrS_3$ (B) EDX mapping of a clump of nanomaterials on a TEM sample. (C) TEM images of the nanoparticles, with various magnifications as shown by the scale bars in the images. EDX analysis of this sample gave an atomic composition of 53% S, 30% Ba, and 17% Zr. The reason for the particularly high Ba content in this sample is not currently known.

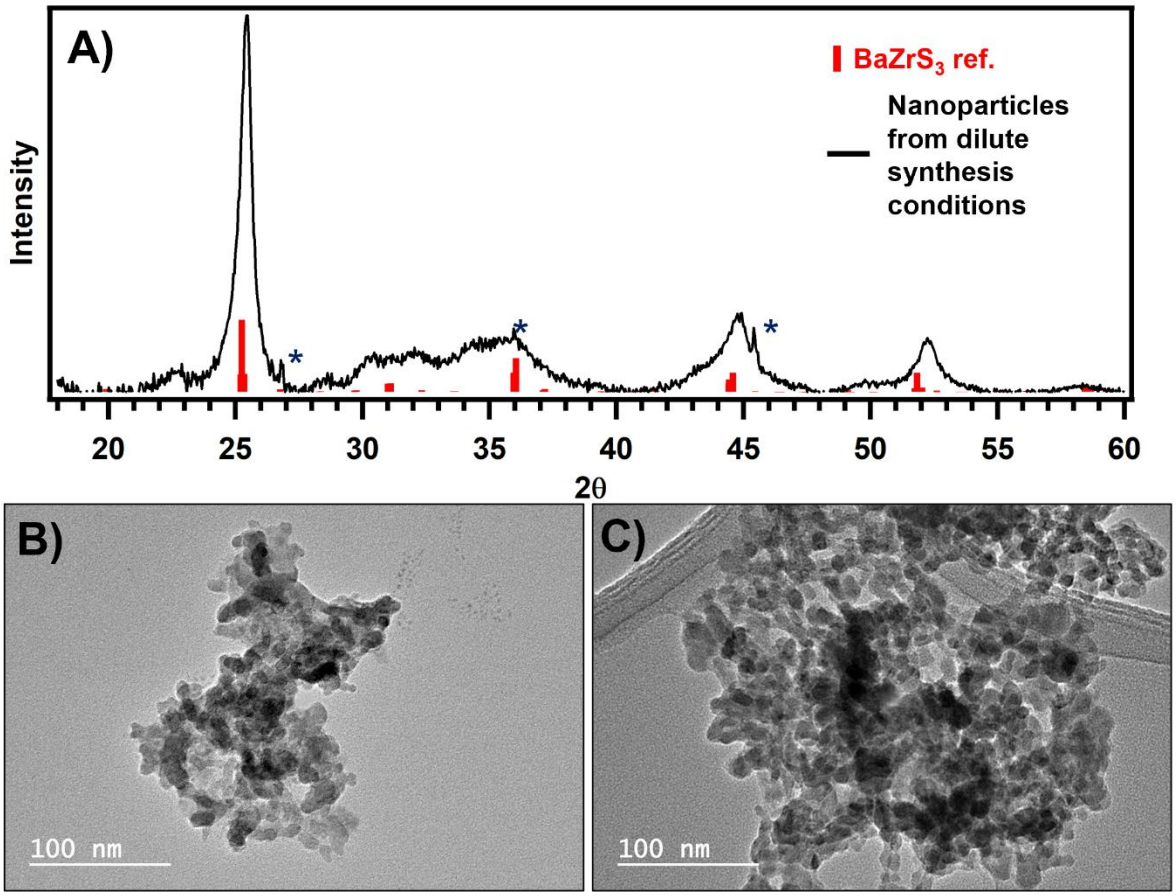

Figure S6. Characterization for $BaZrS_3$ nanomaterials synthesized under dilute conditions; 3 g of oleylamine were used as the reaction solvent rather than 1 g as in the standard conditions. (A) PXRD pattern. Identity of sharp impurity peaks (marked by *) is unknown. (B, C) TEM images of particles. Images were taken on a lacy carbon grid. Some smaller particles, likely an unidentified impurity, can be seen in (B).

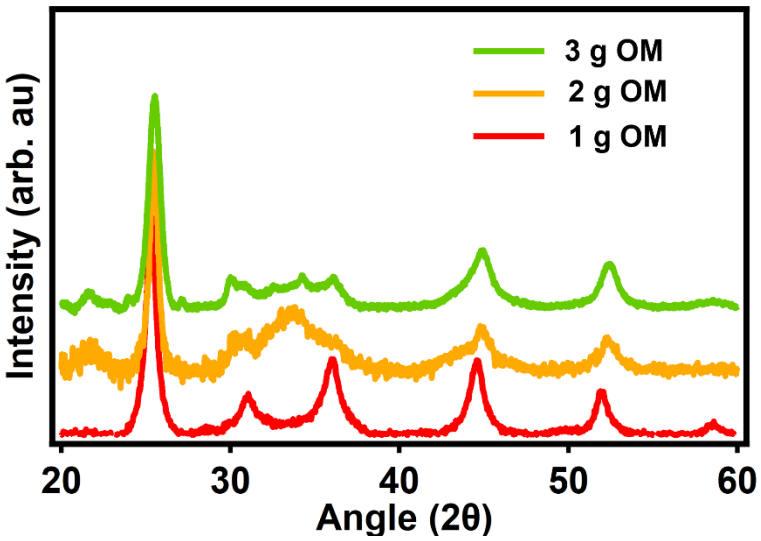

Figure S7. PXRD of the products from reactions carried out at different concentrations (different amounts of oleylamine (OM) solvent).

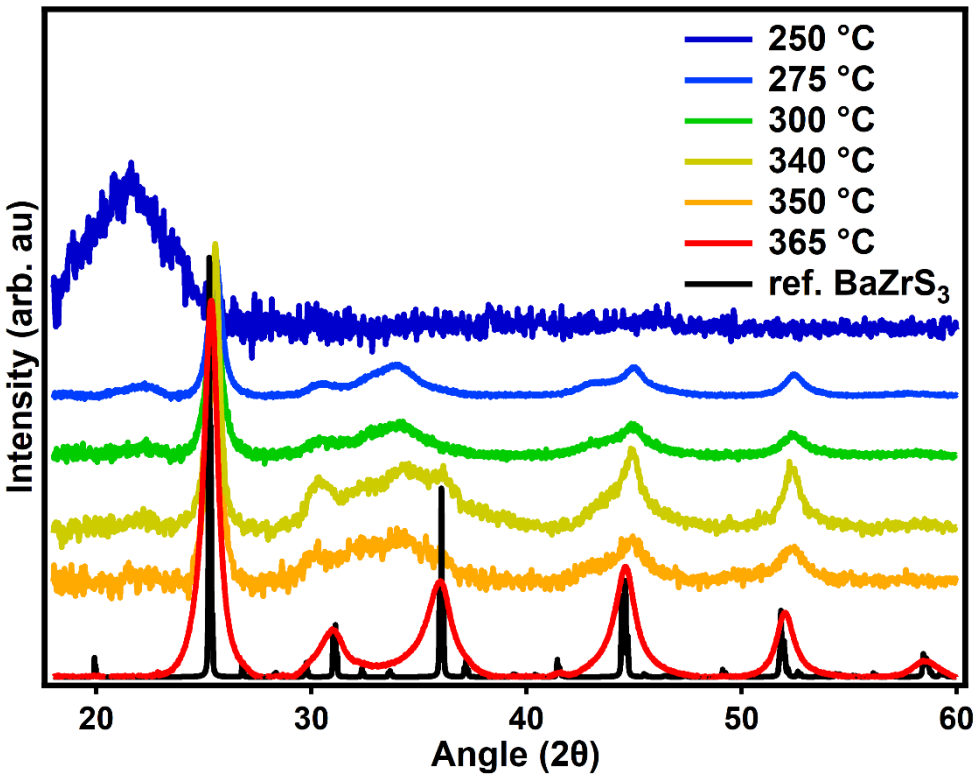

Figure S8. PXRD of the products from reactions carried out at different temperatures.

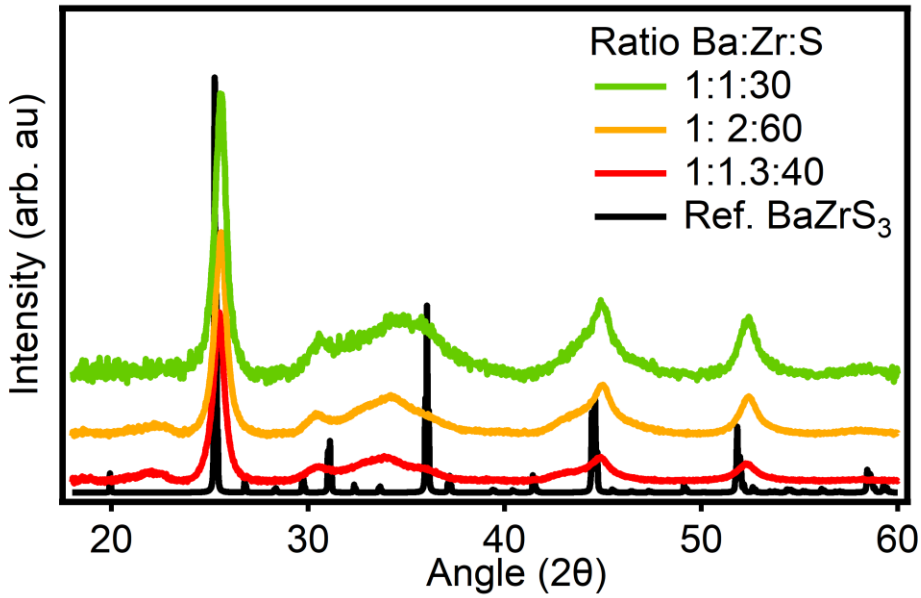

Figure S9. PXRD from $BaZrS_3$ synthesis reactions carried out under standard conditions, but with different mole ratios of Ba:Zr:S (as given in the legend). The reaction carried out with 1:2:60 (yellow curve) represents standard conditions and is an example of a standard reaction that gave "LT-$BaZrS_3$" as a result.

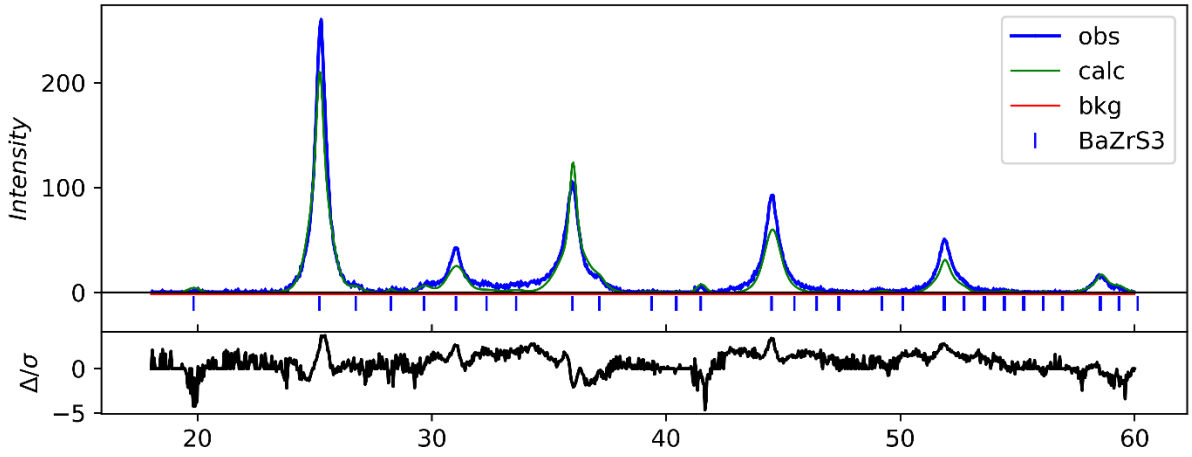

Figure S10. Rietveld refinement of HT-$BaZrS_3$ (sample shown in Figure S5) based on the reported P_{nma} structure. Refinement parameters are shown in the table below. Atomic positions were fixed at the reported values for the bulk structure. The unique axis for uniaxial size broadening and for the March-Dollase parameter was [010].

Table S3. Refinement Parameters Corresponding to Figure S10

Parameter	Fitted Value
a (Å)	7.07774
b (Å)	10.01052
c (Å)	7.08678
U_{iso} (for all atoms)	0.06829
March-Dollase Ratio	0.733
Equatorial size (nm)	34
Axial size (nm)	6
Sample displacement (µm)	283.6
R_w	44.1%

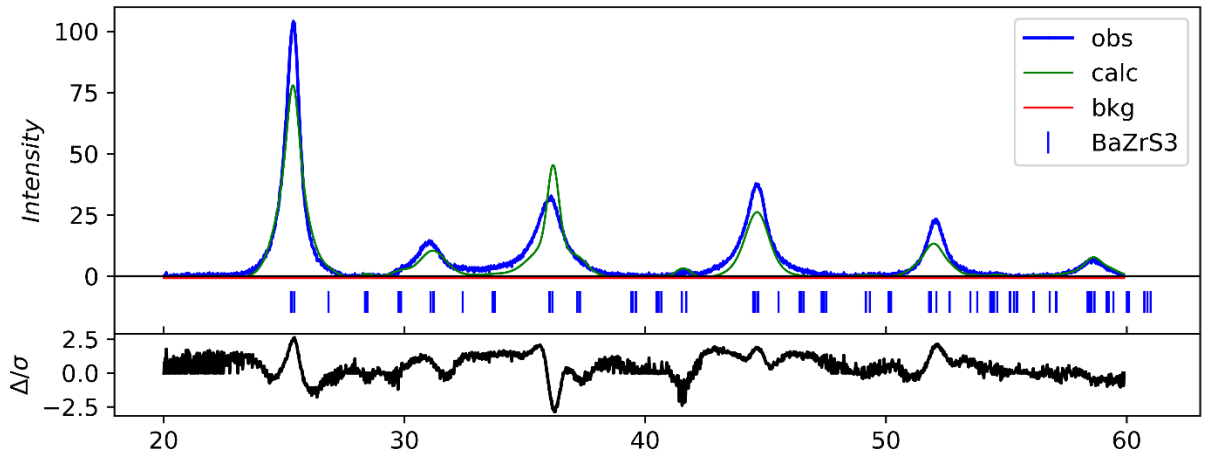

Figure S11. Rietveld refinement of HT-$BaZrS_3$ (sample shown in Figure 2 of the main text) based on the reported P_{nma} structure. Refinement parameters are shown in the table below. Atomic positions were fixed at the reported values for the bulk structure. The unique axis for uniaxial size broadening and for the March-Dollase parameter was [010].

Table S4. Refinement Parameters Corresponding to Figure S11

Parameter	Fitted Value
a (Å)	7.20998
b (Å)	10.20141
c (Å)	7.17139
U_{iso} (for all atoms)	0.05209
March-Dollase Ratio	0.823
Equatorial size (nm)	19
Axial size (nm)	5
Sample displacement (µm)	124.4
R_w	42.7%

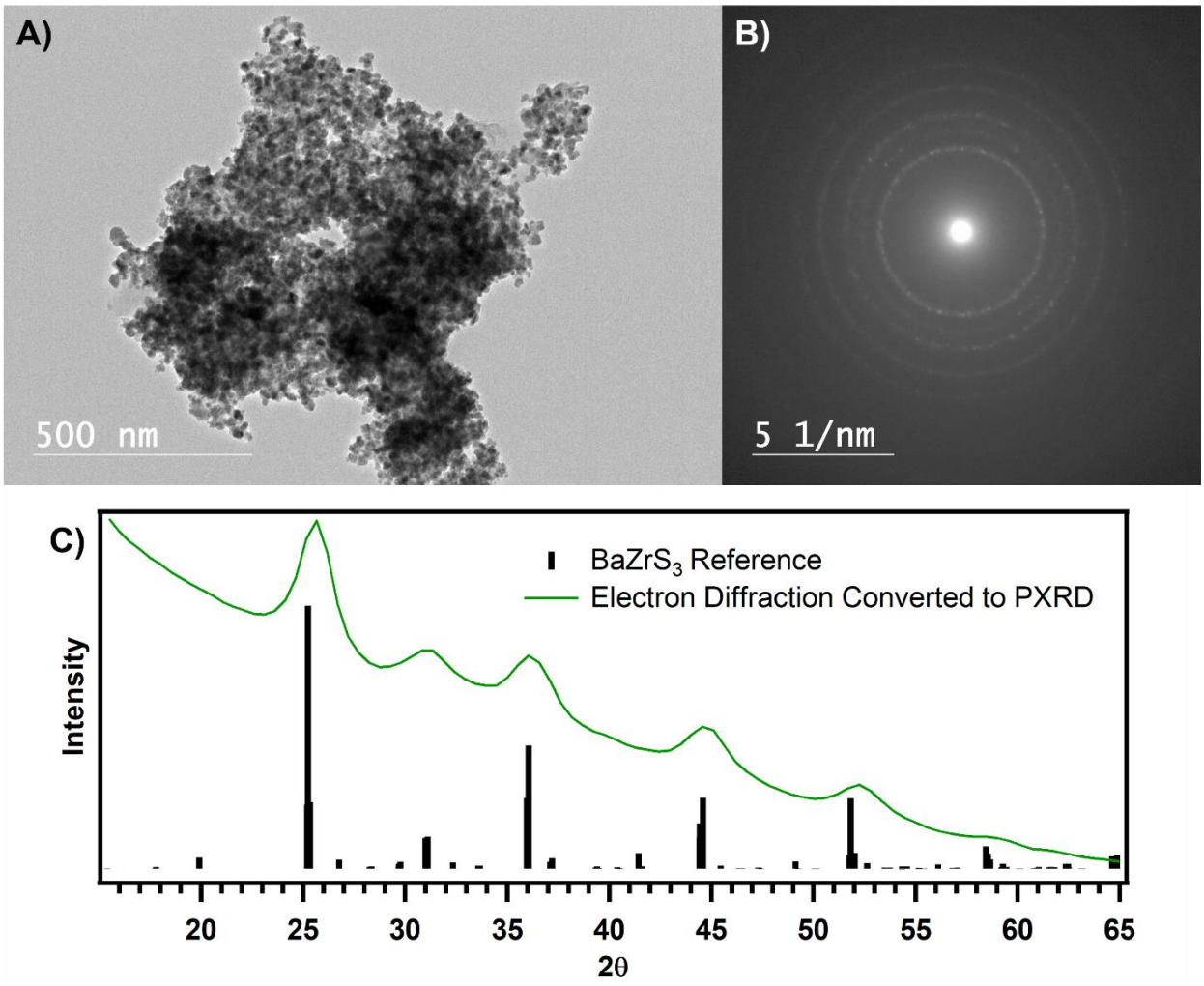

Figure S12. Electron diffraction data and analysis for sample of HT-$BaZrS_3$ (other data for this sample was shown in Figure 2 of the main text). (A) Area of sample (TEM image) from which the electron diffraction was acquired. (B) Electron diffraction rings. (C) Electron diffraction data integrated and converted to a simulated PXRD pattern (Cu Kα radiation) using ED2PXRD,[8] compared to reference.

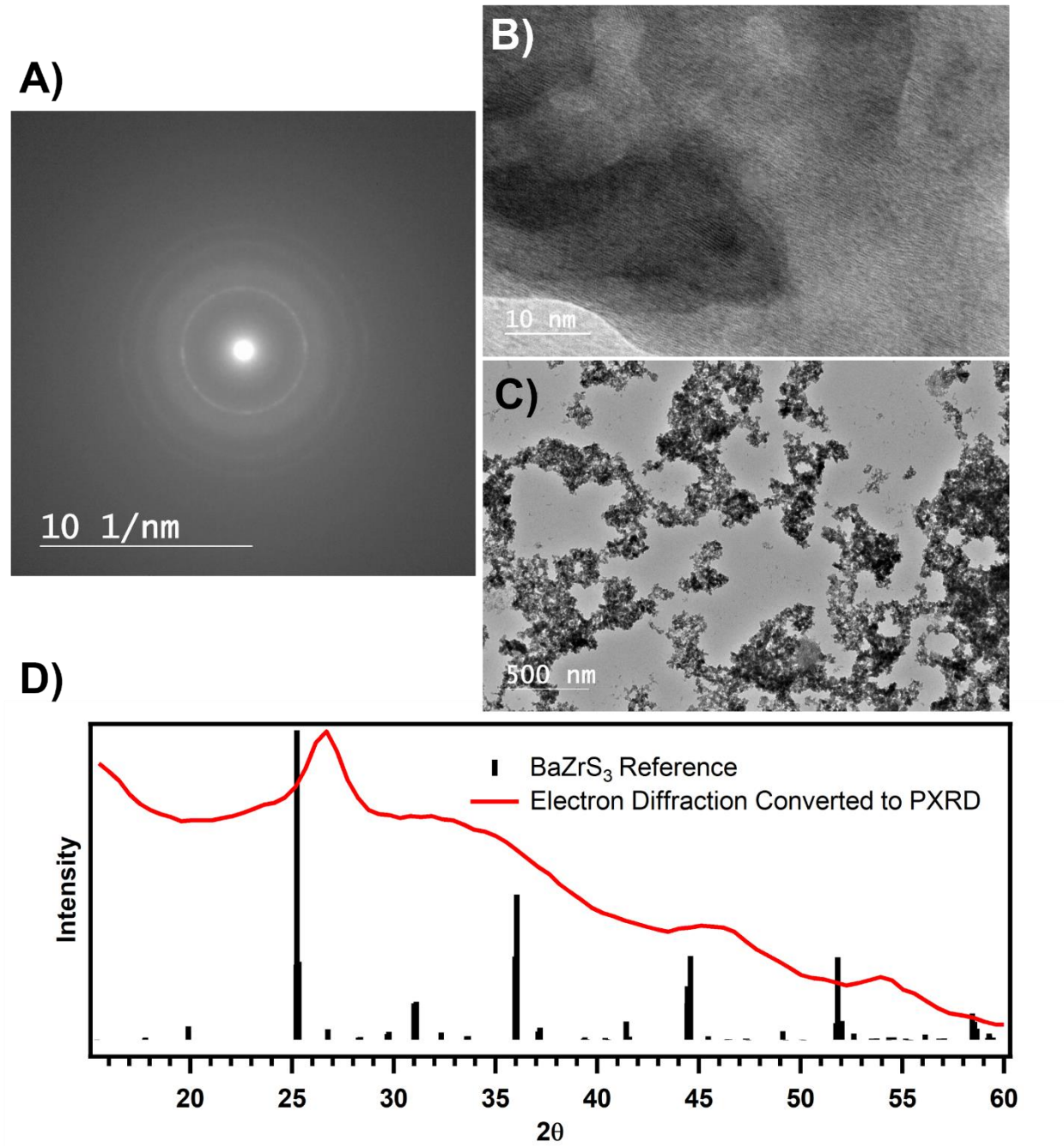

Figure S13. Electron diffraction data and analysis from a sample of LT-$BaZrS_3$.

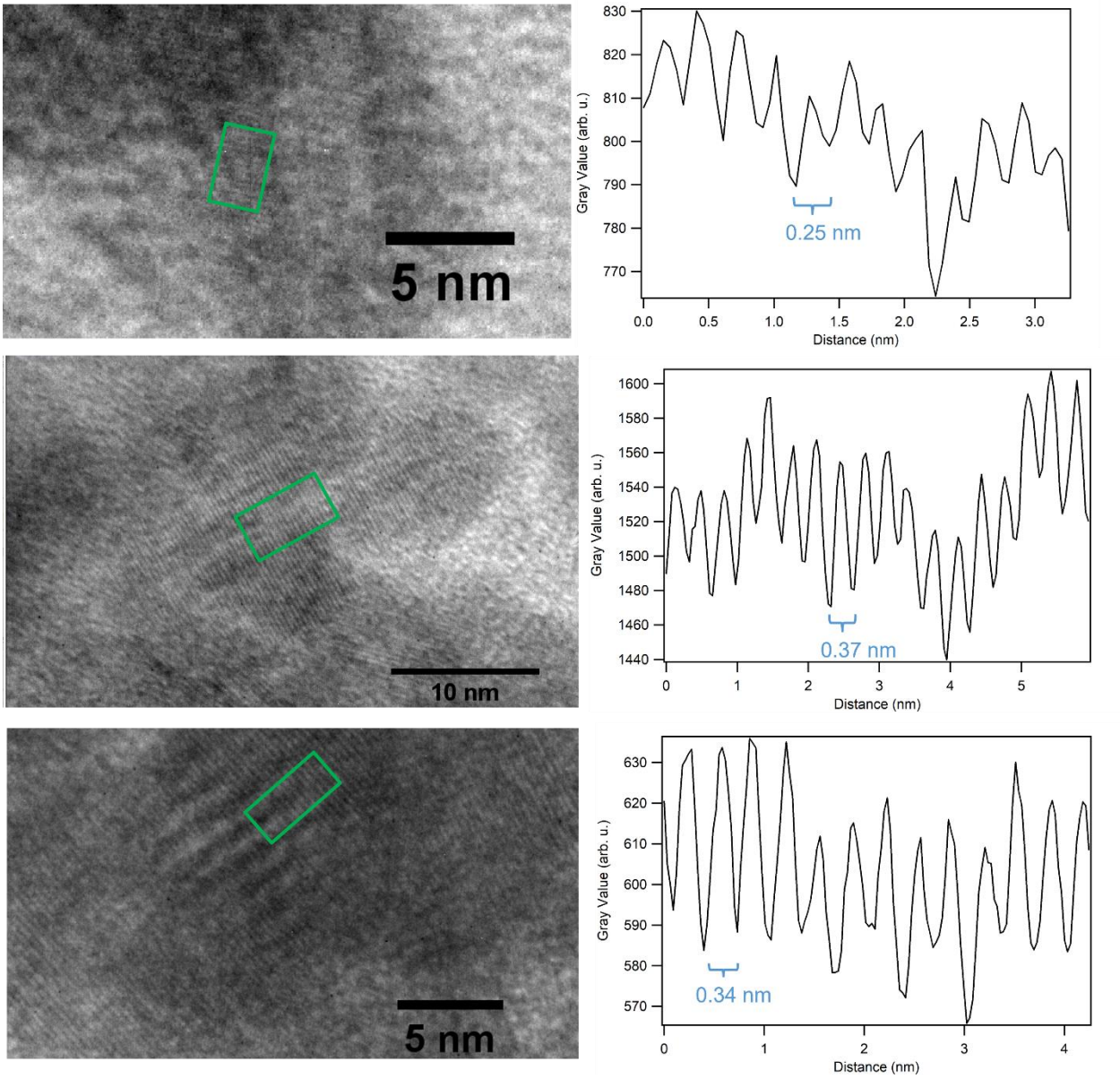

Figure S14. Selected images of $BaZrS_3$ particles showing regions where lattice fringes were visible. For each image, a line profile (averaged over the width of the green box shown on the image) is shown to the right of the image, and the approximate spacing between adjacent fringes is given. In the distorted perovskite $BaZrS_3$ structure, a d-spacing of approximately 0.25 nm would be consistent with either the (040) or (202) lattice planes, which contribute to the prominent diffraction peak observed at $2\theta = 36.0^{o}$ in the Cu K_{α} PXRD. A d-spacing of approximately 0.36±2 nm could be consistent with the (200), (121), or (002) lattice planes which all have about the same spacing and contribute to the prominent diffraction peak observed at about $2\theta = 25.2^{o}$ in the Cu K_{α} PXRD.

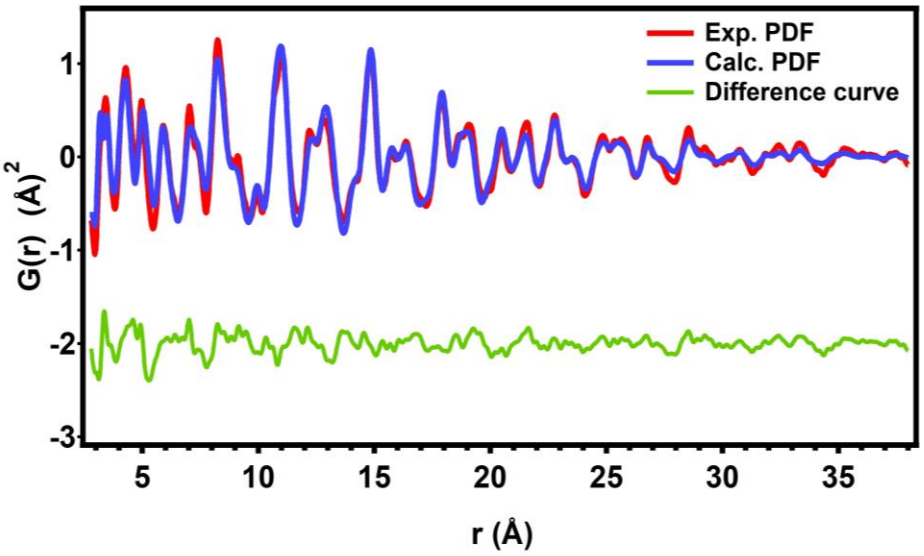

Figure S15. PDF data for HT-$BaZrS_3$ sample, showing fit (to *Pnma* $BaZrS_3$) out to higher ***r***.

Note on Fitting Pair Distribution Function Data: Only the lattice parameters and isotropic displacement parameters on each atom type of the fitted phases were refined (as well as an isotropic nanoparticle size parameter). Atomic positions were kept fixed to their positions in the reference phase. Q_{max} for all samples/fits is 23.8.

Table S5. **PDF refined parameters.**

Sample	**HT-$BaZrS_3$**	**LT-$BaZrS_3$**		
Fitted Phase	$BaZrS_3$ (*Pnma*)	$BaZrS_3$ (*Pnma*)	$Ba_3Zr_2S_7$ ($P4_2/mnm$)	Ba_2ZrS_4 ($I4/mmm$)
a	7.065	7.100	7.057	4.937
b	9.976	9.791	7.057	4.937
c	7.028	7.087	25.371	15.700
scale	0.586	0.802	0.521	0.791
spdiameter	48.83	34.564	40.804	29.918
delta 1	2.019	1.9265	2.050	2.376
U_{iso} *(Ba)*	0.022	0.029	0.0325	0.066
U_{iso} *(Zr)*	0.028	0.058	0.008	0.033
U_{iso} *(S)*	0.030	0.030	0.109	0.222
Q_{damp}	0.046	0.094	0.056	0.092
Q_{broad}	0.001	0.015	0.079	0.007
R_w	42%	42%	64%	68%

Supplemental References.

1 R. L. Kuhlman, B. A. Vaartstra, K. G. Caulton, P. S. Tanner and T. P. Hanusa, in *Inorganic Syntheses*, ed. A. H. Cowley, John Wiley & Sons, Inc., Hoboken, NJ, USA, 2007, pp. 8–10.

2 B. A. Vaartstra, J. C. Huffman, W. E. Streib and K. G. Caulton, *Inorg. Chem.*, 1991, **30**, 121–125.

3 D. Zilevu and S. E. Creutz, *Chem. Mater.*, 2021, **33**, 5137–5146.

4 C. L. Farrow, P. Juhas, J. W. Liu, D. Bryndin, E. S. Božin, J. Bloch, T. Proffen and S. J. L. Billinge, *J. Phys.: Condens. Matter*, 2007, **19**, 335219.

5 E. B. Segal, *Chem. Health Saf.*, 1998, **5**, 25–28.

6 N. E. Ingram, B. J. Jordan, B. Donnadieu and S. E. Creutz, *Dalton Transactions*, 2021, **50**, 15978–15982.

7 V. K. Ravi, S. H. Yu, P. K. Rajput, C. Nayak, D. Bhattacharyya, D. S. Chung and A. Nag, *Nanoscale*, 2021, **13**, 1616–1623.

8 H. Liu, M. Foley, Q. Lin and J. Liu, *J Appl Cryst*, 2016, **49**, 636–641.